



## A Jackknife Estimator of Variance for a Random Tessellated Stratified Sampling Design

Magnussen, Steen; Nord-Larsen, Thomas

*Published in:*  
Forest Science

*DOI:*  
[10.1093/forsci/fxy070](https://doi.org/10.1093/forsci/fxy070)

*Publication date:*  
2019

*Document version*  
Publisher's PDF, also known as Version of record

*Document license:*  
[CC BY-NC](https://creativecommons.org/licenses/by-nc/4.0/)

*Citation for published version (APA):*  
Magnussen, S., & Nord-Larsen, T. (2019). A Jackknife Estimator of Variance for a Random Tessellated Stratified Sampling Design. *Forest Science*, 65(5), 543-547. <https://doi.org/10.1093/forsci/fxy070>

This is an Open Access article distributed under the terms of the Creative Commons Attribution Non-Commercial License (<http://creativecommons.org/licenses/by-nc/4.0/>), which permits non-commercial re-use, distribution, and reproduction in any medium, provided the original work is properly cited. For commercial re-use, please contact [journals.permissions@oup.com](mailto:journals.permissions@oup.com)

biometrics

# A Jackknife Estimator of Variance for a Random Tessellated Stratified Sampling Design

Steen Magnussen<sup>○</sup> and Thomas Nord-Larsen<sup>○</sup>

Semisystematic sampling designs—in which a population area frame is tessellated into cells, and a randomly located sample is taken from each cell—affords random tessellated stratified (RTS) Horvitz–Thompson-type estimators. Forest inventory applications with RTS estimators are rare, possibly because of computational complexities with the estimation of variance. To reduce this challenge, we propose a jackknife estimator of variance for RTS designs. We demonstrate an application with a model-assisted ratio of totals estimator and data from the Danish National Forest Inventory. RTS estimators of standard error were, as a rule, smaller than comparable estimates obtained under the assumption of simple random sampling. The proposed jackknife estimator performed well.

**Keywords:** semisystematic sampling, spatial balance, National Forest Inventory, model-assisted ratio of totals estimator, LiDAR, auxiliary variables

Horvitz–Thompson (HT)-type estimators of a population total and variance have been proposed for single-stage semisystematic sampling designs in which one or more sample locations are selected at random within each of  $N$  spatial units tessellating the sample frame of a population for which one or more study variables ( $Y$ ) are the focus of our interest (Cordy 1993, Stevens and Olsen 2003). Published accounts of practical applications are still few, and in forestry they may be limited to an example with two-stage sampling (Fattorini et al. 2009). When only one randomly located sample unit is selected in each spatial unit, the design goes under the name of random tessellated stratified (RTS) sampling design coined by Stevens and Olsen (2003). An example from the Danish National Forest Inventory is provided in Figures 1 and 2. The HT-type variance estimator for RTS involves complex spatial computations that may deter large-scale applications. Simpler, replicate estimators of variance (Wolter 2007, ch. 4–5) have not yet emerged. In this study, we extend the HT-type estimators for an RTS design to a model-assisted ratio of totals, and we propose a jackknife RTS estimator of variance. An application example from the Danish National Forest Inventory 2012–16 (Magnussen et al. 2018) with data on wood volume and forestland is given.

## Materials and Methods

### National Forest Inventory Sampling Design

The Danish National Forest Inventory (NFI) is a continuous inventory, with partial replacement of sample plots located at random

within cells of a  $2 \times 2$ -km (400 hectares) grid covering the entire country. The sampling frame is the land surface of Denmark (Nord-Larsen and Johansen 2016). Approximately one-third of the sample plots are permanent and re-measured in every cycle of the NFI, whereas two-thirds are temporary with a new (random) location chosen in advance of a measurement. Sample plots are geographically distributed into five nonoverlapping and spatially balanced interpenetrating panels (Kish 1998, Olsen et al. 1999, McDonald 2003, Zhang et al. 2003). Each year, within a 5-year cycle, a different panel is measured. Each sample plot is composed of four circular subplots with a radius of 15 m and located in the corners of a  $200 \times 200$  m square. Centers of subplots are all in the same cell as the plot center. The current inventory cycle includes  $n = 15,137$  sample locations in cells with a land surface area. Subplots with a center in open water (approximately 4 percent) are dropped.

Only plots likely to contain forest or other wooded land are subject to a field visit. This includes plots with forest in the most recent past field visit. The decision to visit or not is based on interpretation of aerial photos by a trained interpreter. To avoid errors of omissions, the interpretation included a 15–20-m buffer zone around each subplot. Administrative records and other auxiliary information served to locate recent afforestation. In the current inventory cycle, 7,185 subplots had a forest cover greater than 2 percent of a subplot area (the minimum registered forest area). Field data from 487 subplots, predominantly in wetlands, were coded as missing (Magnussen et al. 2018). They are treated as missing by design.

Manuscript received June 25, 2018; accepted January 8, 2019; published online March 12, 2019

**Affiliations:** Steen Magnussen ([steen.magnussen@canada.ca](mailto:steen.magnussen@canada.ca)), Natural Resources Canada, Canadian Forest Service, Pacific Forestry Center, 506 West Burnside Road., Victoria, BC V8Z 1M5, Canada. Thomas Nord-Larsen ([tml@ign.ku.dk](mailto:tml@ign.ku.dk)), University of Copenhagen, Faculty of Science.

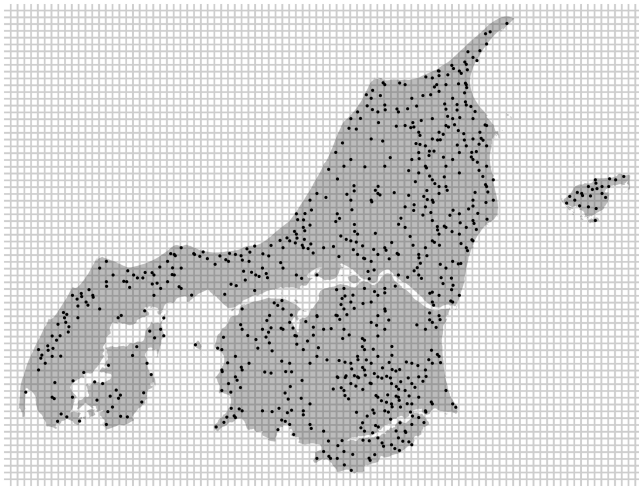


**Figure 1.** Example of RTS sampling design with 727 plot locations in the Danish Region 5 (Nordjylland). Note only plot locations with areas in forest are shown. The  $2 \times 2$  km sampling grid is indicated. The outline of the land surface in Region 5 is indicated by the grayed area.

### Wood Volume

Data collected in a subplot and the calculations of wood volume ( $V$ ,  $m^3$ ) are detailed in Nord-Larsen and Johansen (2016). The sum of subplot wood volumes and forest areas ( $fa$ ) are the response variables of interest for a given sample plot. The forest area ( $fa$ ) was determined geometrically. By definition,  $V$  and  $fa$  are zero in nonvisited plots.

### Predictions of Wood Volume Density

With the aim to reduce the variance in estimators of wood volume density on forest land ( $VOL$   $m^3$   $ha^{-1}$ ), we employ a model-assisted ratio of totals estimator with predictions of  $VOL$  in every sample plot and predictions of totals for the country and regions domains of interest.

The model was based on field data from 2,441 subplots and an airborne laser scanner survey of Denmark (2014–15) with a Riegl LMS-680i scanner in a fixed-wing aircraft (Nord-Larsen et al. 2017). The working model (sensu Särndal et al. 1992, ch. 6.7) was:

$$\hat{VOL} = 15.7277 \times Dz_{\text{mean}12}^{1.2254} \times Dz_{p95,12}^{-0.0138} \times IR_1^{0.9049} \quad (1)$$

where  $Dz_{\text{mean}12}$  is the mean height above ground of first returns (exclusive returns from  $<1$  m above ground),  $Dz_{p95,12}$  is the height above ground of the 95th percentile of first returns (exclusive returns from  $<1$  m above ground), and  $IR_1$  is the interception ratio (ratio of pulses reflected from above ground [ $>1$  m] of first return pulses to the total number of emitted pulses). The relative root mean squared error of the regression was 41 percent (Nord-Larsen et al. 2017, Table 4).

Country and domain totals of  $V$  and  $fa$  were obtained via a summation of wall-to-wall map predictions of  $VOL$  and forest area with  $25 \times 25$  m pixels (Nielsen et al. 2014, Nord-Larsen et al. 2017). The full area of a pixel ( $625$   $m^2$ ) was classified to forest or nonforest. The summation was over  $N_{25 \times 25}^{\text{for}} = 10,196,844$  forested pixels.

### RTS Estimators

Following Cordy (1993) and Stevens (1997), an RTS HT type model-assisted estimator of  $VOL$  becomes

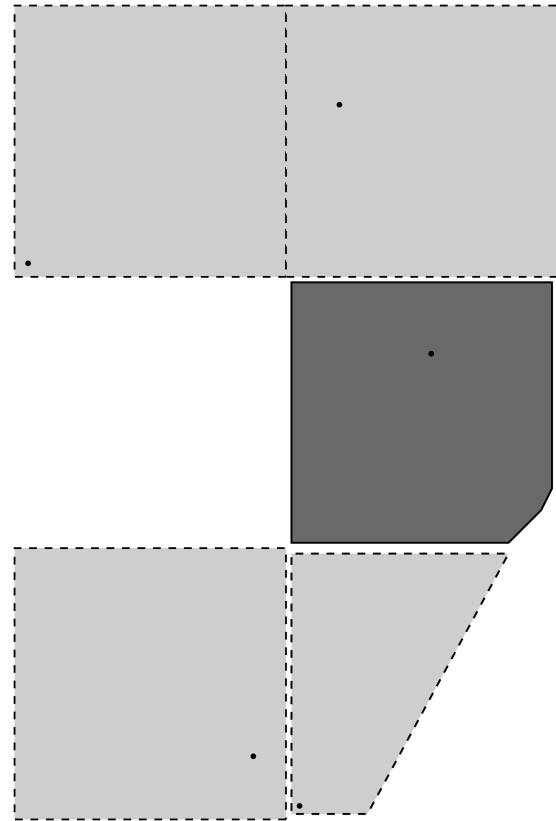


**Figure 2.** Enlargement of the south-western corner of Region 5 (cf. Figure 1).

$$\begin{aligned} \hat{VOL}^{\text{RTS}} &= \hat{VOL}^{\text{SYN}} + \left( \frac{\hat{t}_{wV}}{\hat{t}_{wfa}} - \frac{\hat{t}_w \hat{V}}{\hat{t}_w \hat{fa}} \right) \\ &= \frac{t_{\hat{V}}}{t_{fa}} + \frac{\sum_{i=1}^n \hat{e}_i \times w_i}{\sum_{i=1}^n \hat{t}_{fa_i} \times w_i} = \frac{t_{\hat{V}}}{t_{fa}} + \hat{R}_{we} \\ \hat{VOL}^{\text{SYN}} &= \frac{t_{\hat{V}}}{t_{fa}} = \left( \frac{N_{25 \times 25}^{\text{for}} \hat{VOL}_{25^2}}{10,000} \right) \left( \frac{N_{25 \times 25}^{\text{for}} 25^2}{\sum_{p=1}^{N_{25 \times 25}^{\text{for}}} 25^2} \right)^{-1} \quad (2) \\ \hat{t}_{wV} &= \sum_{i=1}^n VOL_i \times w_i \\ \hat{t}_w \hat{V} &= \sum_{i=1}^n \hat{VOL}_i \times w_i \\ \hat{t}_{wfa} &= \sum_{i=1}^n fa_i \times w_i \\ \hat{e}_i &= VOL_i - \hat{VOL}_i \\ w_i &= \min(\text{land area in hectares in the } i\text{th inventory cell, } 400) \end{aligned}$$

### Management and Policy Implications

Many national forest inventories continue to employ estimators for simple random sampling, even when the sampling design is semisystematic and allowing for potentially more efficient estimators that may capture the variance lowering effects of a spatial covariance process operating at the scale of observation. The RTS HT-type estimators used in this study with data from the Danish National Forest Inventory are one such example. To reduce computational efforts required with RTS estimators, we propose a jackknife RTS estimator of variance that worked well in our case study and also easy to implement.

where  $\hat{V}OL^{SYN}$  is the model-based ratio of totals ( $t_v$  and  $t_{fa}$ ) estimator,  $\hat{t}_{wV}$  an HT-type design-based estimator of the country total of VOL,  $\hat{t}_{w\hat{V}}$  the HT-type design-based estimator of the total of  $\hat{V}OL$ , and  $\hat{t}_{wfa}$  the HT-type design-based estimator of the total forest area. The subscript  $w$  is for sampling intensity (weight), which (here) is the inverse of the land area in a  $2 \times 2$  km cell (400 hectares). In the second r.h.s. expression,  $e_i$  is the difference (residual) between the observed plot value of VOL and the model-based prediction  $\hat{V}OL$ , and  $t_{fa_i}$  is the total forest area in the  $i$ th plot.

Land areas in a cell were computed by integration after overlaying the  $2 \times 2$  km national grid on land polygons at a scale of  $1:2 \times 10^6$  downloaded from Kortforsyningen (<https://kortforsyningen.dk/>, accessed April 18, 2018).

The HT-type model-assisted RTS estimator of VOL is shown in Equation 3:

$$\begin{aligned} \hat{V}ar \left( \hat{V}OL^{RTS} \right) &= \hat{V}ar \left( \frac{\sum_{i=1}^n \hat{e}_i \times w_i}{\sum_{i=1}^n t_{fa_i} \times w_i} \right) \cong \sum_{i=1}^n \sum_{j=1}^n \ddot{\Delta}_{ij} w_i w_j \hat{e}_i \hat{e}_j \\ &+ \hat{R}_{we} \sum_{i=1}^n \sum_{j=1}^n \ddot{\Delta}_{ij} w_i w_j t_{fa_i} t_{fa_j} - \\ &\quad 2 \hat{R}_{we} \hat{C}OV \left( \sum_{i=1}^n w_i \hat{e}_i, \sum_{i=1}^n w_i t_{fa_i} \right) \\ &\cong \sum_{i=1}^n \sum_{j=1}^n \ddot{\Delta}_{ij} w_i w_j \hat{e}_i \hat{e}_j + \hat{R}_{we}^2 \sum_{i=1}^n \sum_{j=1}^n \ddot{\Delta}_{ij} w_i w_j t_{fa_i} t_{fa_j} \\ &- 2 \hat{R}_{we} \sum_{i=1}^n \hat{C}OV \left( w_i \hat{e}_i, w_i t_{fa_i} \right) \end{aligned} \quad (3)$$

where  $\ddot{\Delta}_{ij} = 1 - w_i w_j w_{ij}^{-1}$ ,  $\ddot{\Delta}_{ii} = 1 - w_i$ , and  $w_{ij}$  is the joint sampling intensity for plots  $i$  and  $j$ . In finite populations, the concept of the joint sample inclusion probability of two population units is intuitive and easy to compute for most sampling designs relevant in forest inventories (Särndal et al. 1992, ch. 2.4). The joint sampling intensity in RTS is the relative frequency with which two randomly selected sample locations would occupy the same cell under all possible starting-points of the random sampling grid (i.e., points within a  $2 \times 2$  km cell). Technically, the computations follow the same geometric principles used to compute the joint sample inclusion zone of two trees (Gregoire and Valentine 2008, ch. 10). To wit,  $w_{ij}$  is computed as  $|A_i \cap A_j| \times \left( \frac{1}{|A_{ij}|} - |A_i \cap A_j| \right)^{-1}$  (Stevens 1997) where  $|A_i \cap A_j|$  is the area of overlap between the land polygons—centered on their respective plot locations—in cells with the  $i$ th and  $j$ th plot. Overlap of land polygons in a regular grid is restricted to the eight adjoining neighbors to a  $4 \text{ km}^2$  cell. Figures 3 and 4 illustrate the geometric principles for computing overlap areas. In the above ratio of totals estimator, summations can be limited to cells with forestland.

### A Jackknife RTS Estimator of Variance

The HT-type RTS variance estimator is complex with potentially many taxing computations of overlapping areas. As an alternative, we propose a leave-one-out jackknife estimator of variance (Wolter 2007, ch. 4) for RTS sampling designs. First, we compute the  $n$  pseudovalues of the RTS estimator of VOL given in Equation 2 without the plot totals from the  $i$ th plot,  $i = 1, \dots, n$ . The pseudovalues are in Equation 4 where subscript  $-i$  indicates that data from the  $i$ th plot have been dropped, and  $w_{i'}^*$  is an adjusted weight for the  $i'$ th plot.

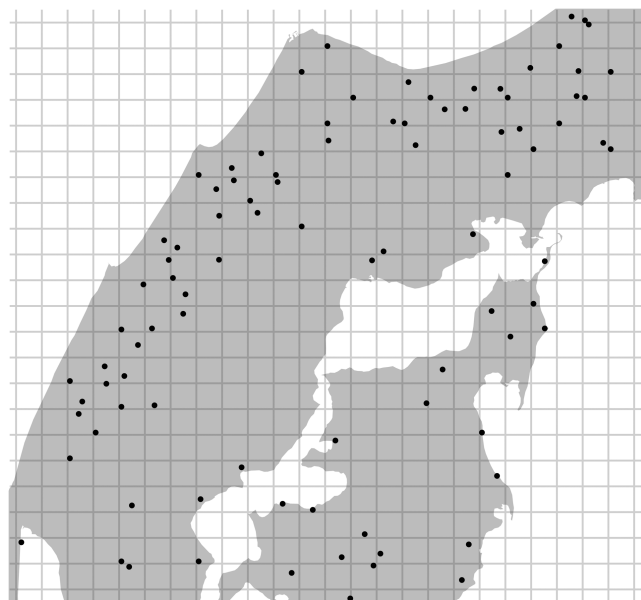


Figure 3. Land area polygons of a focus plot (dark gray, full outline) and its four forested nearest neighbor plots (light gray and dashed outline). Random plot locations are indicated (black dots).

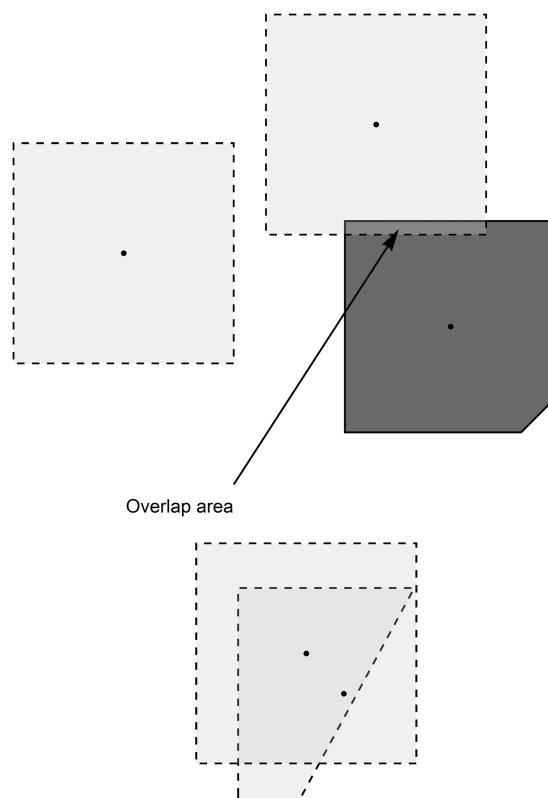


Figure 4. Land area polygons in Figure 3 following a centering on the respective plot locations. A single overlap area of the land area polygon of the focus plot and its northern neighbor is indicated.

$$\hat{V}OL_{-i}^{RTS} = \frac{t_{\hat{V}}}{t_{fa}} + \frac{\sum_{i' \neq i} e_{i'} \times w_{i'}^*}{\sum_{i' \neq i} t_{fa_{i'}} \times w_{i'}^*} = \frac{t_{\hat{V}}}{t_{fa}} + \hat{R}_{w^*e}, \quad i', i = 1, \dots, n \quad (4)$$

The adjusted weight given to the  $i'$ th plot is the inverse of the sum of the land area in the  $i'$ th grid cell and the part of the land

area in the dropped cell ( $i$ ) closer to the  $i'$ th grid cell centroid than to any other grid cell  $j \neq i$ . The reweighting followed the jackknife method for unequal probability sampling in finite populations (Wolter 2007, ch. 4.3.4, Valliant and Dever 2018, p. 83). In short, the cell area of a deleted plot is first divided into four equal parts (equilateral triangles) (Okabe et al. 2000), and subsequently the land area within each of the four triangles is added to the land area of the four first-order neighbors to the deleted plot. The regular grid, plus the fact that 84 percent of the cells covering a part of Denmark had the maximum possible land area of 4 km<sup>2</sup>, accelerated the computation of adjusted weights. The mean of the  $n$  pseudovalues in Equation 4 is our jackknife model-assisted ratio of totals estimator of VOL.

The proposed standard jackknifed estimator of variance (Wolter 2007, p. 166) was hereafter

$$\hat{\text{Var}}_{JK}(\hat{\text{VOL}}^{\text{RTS}}) = n^{-1}(n-1)^{-1} \sum_i^n \left( \hat{\text{VOL}}_{-i}^{\text{RTS}} - \bar{\text{VOL}}_{-i}^{\text{RTS}} \right)^2 \quad (5)$$

where  $\bar{\text{VOL}}_{-i}^{\text{RTS}}$  is the average of the  $n$  pseudovalues  $\hat{\text{VOL}}_{-i}^{\text{RTS}}$ ,  $i = 1, \dots, n$ .

Estimators 2–5 were computed for Denmark (DK) and five administrative regions (here: R1–R5) considered as poststrata. Regional estimates were, in each case, obtained by an evaluation over plots with a majority of subplots within the region of interest. The variance from the random number of sample plots in a region was ignored; it is an order of magnitude smaller than the sampling error (Cochran 1977, ch. 5A.9). Computations were carried out using Mathematica software version 11.3 (Wolfram 2016).

## Results and Discussion

Estimates of wood volume densities and standard errors obtained with the RTS estimators and the jackknife RTS estimator of variance are listed in Table 1. The national RTS estimate of wood volume density was very similar to the estimate obtained with a model-assisted ratio of totals estimator for simple random sampling (SRS) (Magnussen et al. 2018). Regional RTS and SRS estimates of wood volume density also agreed to within 1 percent. Jackknife estimates of wood volume density were, to within 0.6 m<sup>3</sup> ha<sup>-1</sup>, identical to the RTS estimates.

A close agreement between RTS and SRS estimates of volume density was not entirely expected because the sampling weights differ. With a correlation of weights of just 0.27, one could be justified to anticipate practically important differences in estimates of wood volume density. In RTS, the mean land surface area in a 4 km<sup>2</sup> square grid cell was 380 hectares, and the proportion of cells

(plots) with the maximum possible surface area was 0.84. These statistics varied among regions from 370 to 386 hectares, and from 0.77 to 0.89, respectively. The minimum land area was 0.6 hectares, and within regions the minima varied from 0.6 (R5) to 15.7 (R3).

The national RTS estimate of standard error was 1.7 m<sup>3</sup> ha<sup>-1</sup> or just 6 percent below the MA estimate under the assumption of SRS with multiple imputation of missing values. A larger reduction was expected, given the spatial balance in the DNFI data, and the anticipated conservative nature of an SRS estimator (Fuller 1970, Matérn 1980, Sherman 1996, Fewster 2011). In populations with either a spatial covariance process with a range greater than the average interplot distance, or shared regional effects (Dalenius et al. 1961, Bellhouse 1977), the RTS estimator will, in theory at least, generate a lower estimate of variance than an SRS estimator. This follows from the expression in Equation 4 where the covariance arising from the sum of products over neighboring cells is zero in the absence of an overlap among nearest-neighbor sample-location-centered land area polygons. Combined, the small forest sizes, the fragmented nature of forest cover, and a high level of within-forest variation in wood volume densities sets the stage for the similarity of the RTS and SRS estimators of uncertainty. In our data, only 9 percent of the sample plots had three or four nearest neighbors with forest areas in at least one subplot, and 24 percent had no nearest-neighbor plots with a nonzero forest area. To a plot with a forest area, the mean number of neighboring plots with forest was 1.2. Our proposed jackknife estimator of error was 1.8 m<sup>3</sup> ha<sup>-1</sup> and matched the SRS estimator (Magnussen et al. 2018).

Regional estimates of error were more variable—as expected from the reduced sample sizes—but overall they support the notion that RTS and SRS estimates are, from a practical perspective, very similar (Table 1). The proposed jackknife estimator generated estimates that were even closer to the SRS estimates of error.

Although we observed a correlation of forest areas of 0.07 among forested first-order neighbor plots, and a correlation of 0.26 for wood volume, these correlations—in combination with the low number of neighboring forested plots—did not translate into a tangible lowering of the RTS estimate of variance in a model-assisted ratio of totals relative to the variance obtained with an SRS estimator for the same ratio. A larger reduction is anticipated in estimators that do not exploit auxiliary variables (Opsomer et al. 2012, Grafström et al. 2014). The similarity of RTS and SRS estimates of uncertainty does not preclude that they are both overestimating uncertainty in replicated sampling with the RTS design. To obtain further insight on this issue, we would need to simulate replicated sampling from a population intended as a replica of the actual population (Bartolucci and Montanari 2006, Opsomer et al. 2012).

**Table 1. Summary of national (DK) and regional (R1–R5) wood volume density estimates and standard errors (all results in m<sup>3</sup> ha<sup>-1</sup>).**

	DK	R1	R2	R3	R4	R5	Estimator
Plots with forest	4,390	304	668	1,223	1469	727	
$\hat{\text{VOL}}^{\text{RTS}}$	211	290	286	162	199	206	2
$\sqrt{\hat{\text{Var}}(\hat{\text{VOL}}^{\text{RTS}})}$	1.7	5.5	4.6	2.5	2.6	5.5	3
$\hat{\text{VOL}}_{jk}^{\text{RTS}}$	211	290	286	162	199	206	Via 4
$\sqrt{\hat{\text{Var}}_{jk}(\hat{\text{VOL}}_{jk}^{\text{RTS}})}$	1.8	6.3	5.0	3.2	3.0	5.1	5

Practical applications with RTS estimators are still few. Our experience with the DNFI data suggests that with a jackknife RTS estimator of variance, the computational complexities encountered with an RTS HT-type variance estimator become more manageable, even for much larger sampling frames. Applications with more complex tessellations, e.g., hexagons (Bechtold and Patterson 2005) or triangular grids (Mandallaz 2008, ch. 10), do not require new methods.

The use of cell-specific area weights in the HT-type RTS estimators has intuitive appeal when the sample frame is the land surface area of a defined population. A discount for parts of a cell not in the frame is necessary. For countries with long and complex coastal outlines, many area weights may become small, which may lower the design efficiency. If we ignored the land area issue and used the nominal cell area of 4 km<sup>2</sup> as weight, our estimates of standard error would have been 3–5 percent lower.

Our proposed jackknife RTS estimator of variance appears to perform as expected (Shao 1996). In addition to reducing the computational burden, the distribution of  $n$  pseudovalues also provides valuable insights about the influence of individual samples on a final estimate, which may trigger changes to a sampling design and possibly the plot design.

Stevens and Olsen (2003) also proposed an RTS version of a local variance estimator based on the four first-order neighbors to a cell. The estimator shares many attributes with the localized model-based variance estimators (Matérn et al. 1980, Sherman 1996, Ekström and Sjöstedt-de Luna 2004). However, it is not suited for model-assisted ratio of totals estimators as pursued in this study.

## Literature Cited

- BARTOLUCCI, F., AND G.E. MONTANARI. 2006. A new class of unbiased estimators of the variance of the systematic sample mean. *J. Stat. Plan. Inference* 136(4):1512–1525.
- BECHTOLD, W.A., AND P.L. PATTERSON. 2005. *The enhanced forest inventory and analysis program—National sampling design and estimation procedures*. USDA Forest Service Gen. Tech. Rep. SRS-80, Asheville, NC. 85 p.
- BELLHOUSE, D.R. 1977. Some optimal designs for sampling in two dimensions. *Biometrika*. 64:605–611.
- COCHRAN, W.G. 1977. *Sampling techniques*. Wiley, New York. 380 p.
- CORDY, C.B. 1993. An extension of the Horvitz–Thompson theorem to point sampling from a continuous universe. *Stat. Probabil. Lett.* 18:353–362.
- DALENIUS, T., J. HÁJEK, AND S. ZUBRZYCKI. 1961. On plane sampling and related geometrical problems. P. 125–150 in *Proceedings of the 4th Berkeley symposium on probability and mathematical statistics*. University of California, Berkeley, CA.
- EKSTRÖM, M., AND S. SJÖSTEDT-DE LUNA. 2004. Subsampling methods to estimate the variance of sample means based on non-stationary spatial data with varying expected values. *J. Am. Stat. Assoc.* 99(465):82–95.
- FATTORINI, L., S. FRANCESCHI, AND C. PISANI. 2009. A two-phase sampling strategy for large-scale forest carbon budgets. *J. Stat. Plan. Inference* 139:1045–1055.
- FEWSTER, R.M. 2011. Variance estimation for systematic designs in spatial surveys. *Biometrics* 67(4):1518–1531.
- FULLER, W.A. 1970. Sampling with random stratum boundaries. *J. R. Stat. Soc. Series B Stat. Methodol.* 209–226.
- GRAFSTRÖM, A., S. SAARELA, AND L.T. ENE. 2014. Efficient sampling strategies for forest inventories by spreading the sample in auxiliary space. *Can. J. For. Res.* 44(10):1156–1164.
- GREGOIRE, T.G., AND H.T. VALENTINE. 2008. *Sampling strategies for natural resources and the environment*. Chapman & Hall/CRC, Boca Raton, FL. 465 p.
- KISH, L. 1998. Space/time variations and rolling samples. *J. Off. Stat.* 14(1):31–46.
- MAGNUSSEN, S., T. NORD-LARSEN, AND T. RIIS-NIELSEN. 2018. Lidar supported estimators of wood volume and aboveground biomass from the Danish national forest inventory (2012–2016). *Remote Sens. Environ.* 211:146–153.
- MANDALLAZ, D. 2008. *Sampling techniques for forest inventories*. Chapman & Hall, Boca Raton, FL. 251 p.
- MATÉRN, B. 1980. *Spatial variation: Stochastic models and their applications to problems in forest surveys and other sampling investigations*. Springer, New York. 151 p.
- MATÉRN, B., D. BRILLINGER, S. FIENBERG, J. GANI, J. HARTIGAN, AND K. KRICKBERG. 1980. *Spatial variation*. Springer, Berlin. 149 p.
- MCDONALD, T.L. 2003. Review of environmental monitoring methods: Survey designs. *Environ. Monit. Assess.* 85(3):277–292.
- NIELSEN, O.-K., M.S. PLEJDRUP, M. WINTHER, M. NIELSEN, S. GYLDENKÆRNE, M.H. MIKKELSEN, R. ALBREKTSSEN, ET AL. 2014. *Denmark's National Inventory Report 2014. Emission inventories 1990–2012—submitted under the United Nations Framework Convention on Climate Change and the Kyoto Protocol*. Aarhus University, DCE—Danish Centre for Environment and Energy, Århus, Denmark. 1214 p.
- NORD-LARSEN, T., AND V.K. JOHANSEN. 2016. *Danish National Forest Inventory. Design and calculations*. University of Copenhagen, Copenhagen, Denmark. 33 p.
- NORD-LARSEN, T., T. RIIS-NIELSEN, AND M.B. OTTOSEN. 2017. *Forest resource map of Denmark. Mapping of Danish forest resources using ALS from 2014–15*. University of Copenhagen, Copenhagen, Denmark. 18 p.
- OKABE, A., B. BOOTS, K. SUGIHARA, AND S.N. CHIU. 2000. *Spatial tessellations. Concepts and applications of Voronoi diagrams*. Wiley, Chichester, UK. 696 p.
- OLSEN, A.R., J. SEDRANSK, D. EDWARDS, C.A. GOTWAY, W. LIGGETT, S. RATHBURN, K.H. RECKHOW, AND L.J. YOUNG. 1999. Statistical issues for monitoring ecological and natural resources in the United States. *Environ. Monit. Assess.* 54:1–45.
- OPSOMER, J.D., M. FRANCISCO-FERNÁNDEZ, AND X. LI. 2012. Model-based non-parametric variance estimation for systematic sampling. *Scand. J. Stat.* 39(3):528–542.
- SÄRNDAL, C.E., B. SWENSSON, AND J. WRETMAN. 1992. *Model assisted survey sampling*. Springer, New York. 694 p.
- SHAO, J. 1996. Resampling methods in sample surveys. *Statistics*. 27:203–254.
- SHERMAN, M. 1996. Variance estimation for statistics computed from spatial lattice data. *J. Roy. Stat. Soc., Ser. B* 58(3):509–523.
- STEVENS, D.L., AND A.R. OLSEN. 2003. Variance estimation for spatially balanced samples of environmental resources. *Environmetrics* 14(6):593–610.
- STEVENS, D.L.J. 1997. Variable density grid-based sampling designs for continuous spatial populations. *Environmetrics* 8:167–195.
- VALLIANT, R., AND J.A. DEVER. 2018. *Survey weights: A step-by-step guide to calculation*. Stata Press, College Station, TX. 183 p.
- WOLFRAM, S. 2016. *The mathematica documentation center (Version 11.1)*. Wolfram Research, Champaign, IL. 1470 p.
- WOLTER, K.M. 2007. *Introduction to variance estimation*. Springer, New York. 447 p.
- ZHANG, W.Y., Q.W. YAO, H. TONG, AND N.C. STENSETH. 2003. Smoothing for spatiotemporal models and its application to modeling muskrat–mink interaction. *Biometrics* 59(4):813–821.